0026-895X/95/020219-11$3.00/0

MOLECULAR PHARMACOLOGY, 48:219–229 (1995).



# Human Brain-Specific L-Proline Transporter: Molecular Cloning, Functional Expression, and Chromosomal Localization of the Gene in Human and Mouse Genomes

SAAD SHAFQAT, MARIA VELAZ-FAIRCLOTH, VICTOR A. HENZI, KARL D. WHITNEY, TERESA L. YANG-FENG, MICHAEL F. SELDIN, and ROBERT T. FREMEAU, JR.

*Departments of Pharmacology (M.V.-F, V.A.H., K.D.W., R.T.F), Neurobiology (S.S., R.T.F.), Microbiology (M.F.S.), and Medicine (M.F.S.), Duke University Medical Center, Durham, North Carolina 27710, and Department of Genetics, Yale University School of Medicine, New Haven, Connecticut 06510 (T.L.Y-F.)*

Received February 2, 1995; Accepted May 11, 1995

## SUMMARY

L-Proline fulfills several of the classic criteria used to identify amino acid neurotransmitters, including the presence of a high affinity, $Na^+$- (and $Cl^-$)-dependent synaptosomal transport process and the $Ca^{2+}$-dependent release of exogenously loaded radiolabeled L-proline from brain slices and synaptosomes after $K^+$-induced depolarization. However, studies to define the role of L-proline in discrete pathways in the mammalian brain have been precluded by the inability to block its biosynthesis or high affinity transport in nervous tissue. We report the molecular cloning, functional expression, and chromosomal localization of a human brain-specific high affinity L-proline transporter (hPROT). The pharmacological specificity, kinetic properties, and ionic requirements of hPROT clearly distinguish this carrier from the other $Na^+$-dependent plasma membrane carriers that transport L-proline. Multiple tissue Northern blot analysis revealed a prominent ~4-kb mRNA transcript in human brain tissue, whereas no specific hybridizing species were detected in peripheral tissue. An antipeptide antiserum directed against the carboxy-terminus of the predicted hPROT protein identified a single, broad immunoreactive protein of 68 kDa on immunoblots of synaptosomal membranes from various human brain regions. In contrast, no specific labeling was detected on immunoblots of membranes from human liver, kidney, or heart. A differential distribution of hPROT mRNA and protein was observed in the human corpus striatum, consistent with the hypothesis that the hPROT protein is synthesized in neuronal cell bodies in an extrastriatal location and axonally transported to the corpus striatum. These findings warrant the consideration of a synaptic regulatory role for this transporter and its presumed natural substrate, L-proline, in the mammalian central nervous system.

The role of L-proline in the CNS is enigmatic. Although direct evidence is lacking, circumstantial evidence implicates L-proline as a putative synaptic regulatory molecule in the mammalian CNS. In particular, L-proline exhibits several properties similar to those of the well-characterized amino acid neurotransmitters. First, a synaptosomal biosynthetic pathway of L-proline from ornithine has been demonstrated (1). Second, a high affinity $Na^+$-dependent synaptosomal uptake activity has been identified for L-proline (2–4) that exhibits a heterogeneous regional distribution in rodent CNS (5–7). Third, exogenously loaded radiolabeled L-proline is released from neocortical brain slices and synaptosomes in a $Ca^{2+}$-dependent manner after $K^+$-induced depolarization (8, 9). Fourth, specific $Na^+$-independent binding of [$^3$H]-L-proline to rat brain synaptic membranes has been described (10, 11); however, no definitive evidence exists for specific high affinity L-proline receptors in the mammalian CNS. Fifth, L-proline (in millimolar levels) produces complex electrophysiological actions when iontophoresed onto neurons (reviewed in Ref. 12) and inhibits the electrically stimulated release of L-glutamate from rat frontal cortex brain slices (13). Finally, intracerebral injections of L-proline are neurotoxic (14) and disrupt memory processes in chickens (15). Interestingly, the neurotoxic effects of L-proline injections in rat hippocampus are blocked by glutamate receptor antagonists, suggesting that L-proline may be an endogenous excitotoxin (14). These excitotoxic properties of L-proline may contribute to the pathophysiology of type II hyperprolinemia,

This work was supported in part by National Institutes of Health Grants NS32501 (R.T.F.), NRSA NS09463 (L.V.-F.), and HG00734 (M.F.S.) and by National Science Foundation Grant NSF9310965 (R.T.F.).

**ABBREVIATIONS:** PROT, high affinity L-proline transporter; hPROT, human brain-specific high affinity L-proline transporter; rPROT, rat brain-specific high affinity L-proline transporter; CNS, central nervous system; GABA, γ-aminobutyric acid; PCR, polymerase chain reaction; bp, base pair(s); RFLVs, restriction fragment length variants; hnRNA, heterogeneous nuclear RNA; kb, kilobase(s); hSERT, human serotonin transporter gene; SDS-PAGE, sodium dodecyl sulfate-polyacrylamide gel electrophoresis; SBS-T, Tris-buffered saline-Tween 20.

a genetic disorder characterized by elevated plasma and cerebrospinal fluid concentrations of L-proline and a high incidence of childhood seizures (reviewed in Ref. 16).

Definitive studies of the synaptic role of L-proline in discrete brain pathways have not been possible due to the lack of specific inhibitors of the biosynthesis or high affinity transport of L-proline in nervous tissue. Recently, we isolated rat brain cDNA clones for a novel high affinity, $Na^+$- (and $Cl^-$)-dependent PROT (17). *In situ* hybridization of rat brain sections and cultured hippocampal neurons revealed that rPROT mRNA was expressed by subpopulations of glutamatergic neurons in rat brain (17, 18). The substrate specificity, ion dependence, and kinetic properties of the cloned transporter transiently expressed in non-neural cells were similar to the corresponding properties of the synaptosomal high affinity L-proline uptake system in mammalian nervous tissue (4, 17). Sequence analysis and hydropathy profiles revealed that rPROT represented a novel member of the emerging gene family of $Na^+$- (and $Cl^-$)-dependent plasma membrane transport proteins that comprises transporters for several neurotransmitters, including GABA, glycine, norepinephrine, dopamine, serotonin, and transporters for substrates with osmoprotective (taurine, betaine) or metabolic (creatine) roles (reviewed in Ref. 19). These transporters are composed of single polypeptides of ~600 amino acids that exhibit significant amino acid-sequence identities and contain ~12 hydrophobic stretches of 20–26 amino acids that are believed to form transmembrane $\alpha$-helical domains.

In the present study, we describe the molecular cloning, pharmacological characterization, and chromosomal localization of an hPROT. We elucidate several structural features important for high affinity interaction of substrates and/or inhibitors with the hPROT. We also document the brain-specific expression of hPROT mRNA and protein. Furthermore, we report the differential distribution of hPROT mRNA and protein in human corpus striatum, suggesting that the hPROT protein is axonally transported from its site(s) of biosynthesis to nerve terminals in the striatum. These results support a synaptic regulatory role for this transporter and its presumed natural substrate, L-proline, in the mammalian CNS.

## Materials and Methods

**Library screening.** The rPROT cDNA (17) was used as a template in a PCR containing 0.25 mCi of [$^{32}$P]dCTP to generate a 690-bp radiolabeled probe that was used to screen at high stringency a human hippocampal cDNA library in λ-zap (Stratagene, La Jolla, CA). Bluescript plasmids pBSII SK(−) were rescued from plaque-purified positives by *in vivo* excision, as described by the manufacturer (Stratagene). Two populations of positives were identified by restriction analysis, designated HH-1 and HH-2. Nucleotide sequence analysis (Sequenase, US Biochemical Corp., La Jolla, CA) revealed that these human brain cDNAs displayed strong homology with rPROT. HH-1 exhibited homology with the deduced rPROT sequence from amino acids 11–194, followed by several hundred basepairs of unrelated, noncoding sequence that may represent an intron. HH-2 positives displayed homology with the deduced rPROT sequence from amino acid 255 extending to the putative stop codon, followed by several hundred basepairs of 3′-untranslated sequence.

The insert of clone HH-2 was radiolabeled by random priming and used as a probe to screen $1.5 \times 10^6$ recombinants from a human temporal cortex cDNA library in λ-zap (38). A single positive was identified, designated HC-3, that contained a full-length open reading frame coding for a 636-amino acid deduced protein that exhibited ~98% amino acid-sequence identity to rPROT.

Noncoding sequence was removed from clone HC-3 to produce an expression construct designated R44E, which contains the complete coding sequence of the hPROT cDNA with 10 bp of 5′ noncoding region and 70 bp of 3′ noncoding region. To generate R44E, we removed approximately 1500 bp of 3′ untranslated sequence by ligation of *SphI/Xba*I-digested HC-3 to an *SphI/Xba*I-digested PCR product of primers 5′-GCC TCA TGA TCC CAG CTG GCA-3′ and 5′-GCT CTA GAA TCC CAG AGG CA-3′ amplified from HC-3 template; an additional 160 bp of 5′-untranslated sequence were removed by ligation of *KpnI/Sac*I-digested HC-3 to a *KpnI/Sac*I-digested PCR product of primers 5′-GCG GTA CCC ACC CGC TCT CCA AGA TGA A-3′ and 5′-TGC ACC CGC ACC TTT GAA GAG-3′ amplified from HC-3 template. Nucleotide sequence was determined on both strands of the R44E cDNA insert by dideoxynucleotide chain termination (Sequenase, US Biochemical Corp.) using synthetic oligonucleotides as sequencing primers.

**Expression and pharmacological studies.** The full-length R44E cDNA was used for all expression studies described in this report. HeLa cells (100,000–150,000 per well in 24-well plates) were infected with recombinant vaccinia virus strain $VTF_{7-3}$ (1–10 pfu per cell) expressing $T_7$ RNA polymerase, followed 30 min later by liposome-mediated (3 μg per well; Lipofectin, Life Technologies, Gaithersburg, MD) transfection of R44E (1 μg per well) as described (17). Transport assays were conducted 8–9 hr after transfection with 50 nM L-[$^3$H]-proline as substrate in Krebs-Ringer-Tris-HEPES buffer (120 mM NaCl, 4.7 mM KCl, 2.2 mM $CaCl_2$, 10 mM HEPES, 1.2 mM $MgSO_4$, 1.2 mM $KH_2PO_4$, 5 mM Tris; pH adjusted to 7.4). Assays were terminated and washed with ice-cold Krebs-Ringer-Tris-HEPES medium; cells were solubilized with 0.5 ml of 1% SDS; and accumulated radioactivity was determined by scintillation counting. Triplicate control transfections of plasmid vector alone (pBSII SK[−]) were conducted on each 24-well plate to determine background transport values, which were subtracted from signals obtained with hPROT.

**Northern hybridization.** A 1988-bp *KpnI/Xba*I fragment incorporating the full-length hPROT cDNA was radiolabeled with [$^{32}$P] dCTP by random priming (Life Technologies) and hybridized to a human multiple tissue Northern blot and a human multiple brain region Northern blot (both from Clontech, Palo Alto, CA). The hybridization and washing conditions were as described by the manufacturer (Clontech).

**Immunoblotting.** Adult human brain and peripheral tissues were obtained from the Joseph and Kathleen Bryan Alzheimer's Disease Research Center, Duke University Medical Center, Durham, NC. Membranes were prepared and subjected to immunoblotting with an affinity-purified antibody directed against the carboxyl terminus of hPROT (GSQSPKPLMVHMRKYGGITSFENT), designated C-597, as previously described (18). The sensitivity and specificity of this antibody are documented (18). Briefly, tissues were homogenized with a 50-ml glass Teflon motor-driven homogenizer in 10 vol of ice-cold (0–4°) buffer (0.32 M sucrose, 5 mM EDTA, 50 mM HEPES, pH 7.4, and 0.25 mM phenylmethylsulfonyl fluoride) containing the following protease inhibitors: 20 μg/ml trypsin inhibitor, 20 μg/ml benzamidine, 10 μg/ml aprotinin, and 20 μg/ml leupeptin. The homogenates were centrifuged at 800 × *g* for 20 min, and the pellet was discarded. The supernatant was centrifuged at 18,000 × *g* for 30 min, and the resulting pellets, containing crude synaptosomal membranes from various human brain regions or crude plasma membranes from non-neural tissues, were resuspended in 0.5 ml of 20 mM HEPES (pH 7.4). Membranes were assayed for protein content and separated on SDS-polyacrylamide (8%) gels as described (18). Gels were soaked in transfer buffer (250 mM glycine, 50 mM Tris, and 20% methanol) and electroblotted overnight (0.5 A, 4°) to nitrocellulose membranes (Bio-Rad). All subsequent steps were conducted at room temperature. Blots were preincubated (1 hr) in blocking solution of TBS-T (20 mM Tris base, 137 mM NaCl, HCl to pH 7.6, and 0.1% Tween 20) containing 5% nonfat dried milk (Bio-Rad). Blots were

rinsed in TBS-T and then incubated (1 hr) with C597 anti-PROT antibody diluted in TBS-T (0.01 μg/ml). After extensive washing in TBS-T, immunoblots were incubated in peroxidase-linked anti-rabbit antibody (Amersham Corp., Arlington Heights, IL) diluted 1:3000 in TBS-T. Immunoreactivity was detected by exposure to autoradiography film (Kodak), using enhanced chemiluminiscence (ECL, Amersham Corp). Blots were stained with Ponceau S solution (Sigma Chemical Co., St. Louis, MO) to monitor the efficiency of protein transfer. Prestained protein molecular weight markers (Life Technologies, Inc.) were used to estimate the apparent molecular weight of proteins.

**Chromosomal localization of the human and mouse PROT gene.** A mapping panel (panel 1) consisting of 17 mouse-human and one Chinese hamster-human hybrids was obtained from the National Institute of General Medical Sciences Mutant Cell Repository. Characterization of these hybrids and their human chromosome content is described in detail in the National Institute of General Medical Sciences catalog. *In situ* hybridization using tritium-labeled probes of 25 ng/ml to metaphases of a normal individual was conducted as previously described (21).

C3H/HeJ-*gld* and *Mus spretus* (Spain) mice and [(C3H/HeJ-*gld* × *Mus spretus*) F1 × C3H/HeJ-*gld*] interspecific backcross mice were bred and maintained as previously described (22). *Mus spretus* was chosen as the second parent in this cross because of the relative ease of detection of informative RFLVs in comparison with crosses using conventional inbred laboratory strains. DNA isolated from mouse organs by standard techniques was digested with restriction endonucleases, and 10-μg samples were electrophoresed in 0.9% agarose gels. DNA was transferred to Nytran membranes (Schleicher and Schull, Inc., Keene, NH), hybridized at 65°, and washed under stringent conditions. Previous studies have defined the location of the reference loci in the cross used in these studies: *Pdgfrb*, *Grl1*, and *Adrb2* (referenced in Ref. 37). Gene linkage was determined by segregation analysis as previously performed (22). Gene order was determined by haplotype analysis that minimizes crossover frequency among all genes that were determined to be within a linkage group. This method resulted in determination of the most likely gene order (40).

## Results

**Structural features of the hPROT.** The nucleotide and deduced amino acid sequences of the hPROT are shown in Fig. 1. The deduced protein is predicted to have a molecular mass of 70,868 Da and an isoelectric point of 6.58. The hPROT and rPROT are highly similar, sharing ~98% overall amino acid-sequence identity and ~92% nucleotide-sequence identity throughout the open reading frame (Fig. 1). No amino acid-sequence substitutions occur within the putative transmembrane domains of hPROT, relative to rPROT. hPROT is 1 amino acid shorter (636 amino acids) than rPROT (637 amino acids), lacking one of the glutamate residues present at positions 630–634 in the carboxy-terminus of rPROT. Of the 13 remaining differences in amino acid sequence between hPROT and rPROT, 8 occur in the second extracellular loop, 2 occur in the amino-terminus, and 1 each occurs in the carboxy-terminus and the fourth and sixth extracellular loops.

Like the other members of the $Na^+$- (and $Cl^-$)-dependent plasma membrane transporter family, the amino-terminus of hPROT lacks a readily identifiable signal sequence, suggesting that this domain resides on the cytoplasmic face of the membrane. Furthermore, hydropathy analysis predicts the presence of 12 segments of 20–25 hydrophobic amino acid residues that could form transmembrane α-helical domains (Fig. 1), a hallmark of membrane transport proteins. Like its rat counterpart, the hPROT possesses three canonical sites for *N*-linked glycosylation (Asn-39, Asn-182, and Asn-586). However, only Asn-182 is predicted to reside in an extracellular region of the protein, namely, the large hydrophilic loop between putative transmembrane domains 3 and 4. These features of the predicted hPROT protein are consistent with a tentative structural model for this family of transporter proteins that predicts the presence of ~12 transmembrane α-helical domains, cytoplasmic amino- and carboxy-termini, and a large, glycosylated second extracellular loop.

Several consensus sequences for protein kinase-mediated protein phosphorylation (23) are present in putative intracellular domains of hPROT (Fig. 1). These sites are conserved with rPROT and include one consensus site for cAMP-dependent protein kinase phosphorylation, three consensus sites for protein kinase C-dependent protein kinase phosphorylation, and five consensus sites for casein kinase II-dependent phosphorylation (see Fig. 1). Interestingly, the consensus sequence for protein kinase C-dependent protein phosphorylation located in the putative intracellular loop between transmembrane domains 4 and 5 (Ser-239) in hPROT is highly conserved throughout many, if not all, of the transporters in this family (see Fig. 3 in Ref. 19).

**Characterization of the transport properties of hPROT.** To examine the transport properties of the cloned cDNA, we generated an expression construct that contains the complete coding sequence of the hPROT cDNA cloned into the pBluescriptII SK(−) vector such that sense transcription occurs from the $T_7$ promoter (designated R44E). This construct was transfected into HeLa cells expressing $T_7$ RNA polymerase, and [$^3$H]-L-proline uptake was assayed as previously described (17). HeLa cells transiently transfected with the R44E construct express time- and $Na^+$-dependent L-proline uptake (Fig. 2A). Isotonic substitution of extracellular NaCl with choline chloride abolished specific L-proline uptake (Fig. 2A). R44E-induced L-proline uptake was also abolished in chloride-free media (Fig. 2B), confirming that hPROT-induced L-proline transport is $Na^+$- (and $Cl^-$)-dependent, as previously reported for synaptosomal L-proline uptake (24). In contrast, endogenous low affinity ($K_m$ ~350 μM) transport of L-proline in pBluescriptII SK(−)-transfected HeLa cells was dependent on extracellular $Na^+$ but independent of extracellular chloride (Fig. 2B). Fig. 3A shows that L-proline uptake in R44E-transfected HeLa cells is saturable at low substrate concentrations. Eadie-Hofstee transformation of the data yielded a monophasic curve (Fig. 3B) consistent with a single, high affinity interaction with an apparent $K_m$ of 6.2 μM and a maximal velocity ($V_{max}$) of 0.079 fmol/cell/min.

The ability of several proline analogs, amino acids, and related compounds to compete for [$^3$H]-L-proline uptake in hPROT-transfected HeLa cells was examined (Fig. 4 and Table 1). Compounds that inhibited specific L-proline uptake by 50% or more at 100 μM were further evaluated in dose-response experiments, and apparent inhibitor constant ($K_i$) values were determined. hPROT-induced L-proline (50 nM) uptake was stereospecific (Fig. 4 and Table 1). L-Proline inhibited 50 nM [$^3$H]-L-proline transport with a $K_i$ of 7 μM, whereas D-proline exhibited a $K_i$ of ~105 μM. hPROT-induced L-proline uptake was sensitive to pharmacological inhibition by L-pipecolic acid, sarcosine (*N*-methyl-glycine), L-nor-

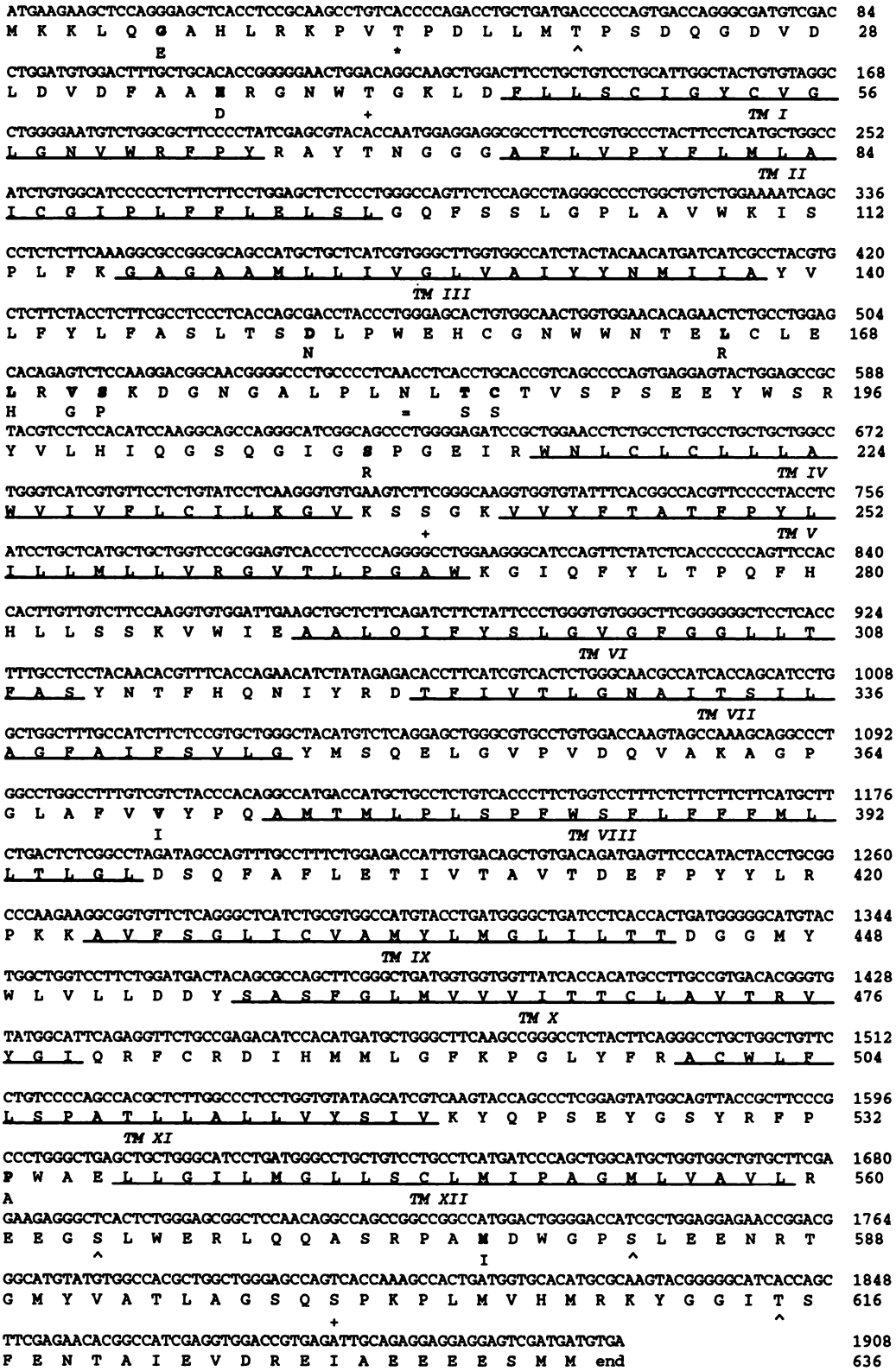


**Fig. 1.** Nucleotide and deduced amino acid sequence of hPROT. The deduced amino acid sequence is shown below the nucleotide sequence. Nucleotides are numbered in the 5′ to 3′ direction beginning with the first residue of the putative initiator methionine. The stop codon flanking the open reading frame is denoted "end." Twelve putative membrane-spanning domains are underlined. Note that the precise boundaries of the transmembrane domains are arbitrary and are drawn for convenience of representation. One potential *N*-linked glycosylation site located on the large putative extracellular loop connecting transmembrane domains 3 and 4 is indicated by *double underlining*. Two additional putative glycosylation sites are located, one each within the putative intracellular $NH_2$- and COOH-terminal domains, and are not shown. *, one potential intracellular consensus sequence for cAMP-dependent protein kinase phosphorylation; +, three putative intracellular consensus sequences for protein kinase C-dependent protein kinase phosphorylation; *caret*, five putative intracellular consensus sequences for casein kinase II-dependent phosphorylation sites. The remaining two protein kinase A sites, two protein kinase C sites, and two casein kinase II sites are located in the putative extracellular domains or within the putative transmembrane domains and are not shown.

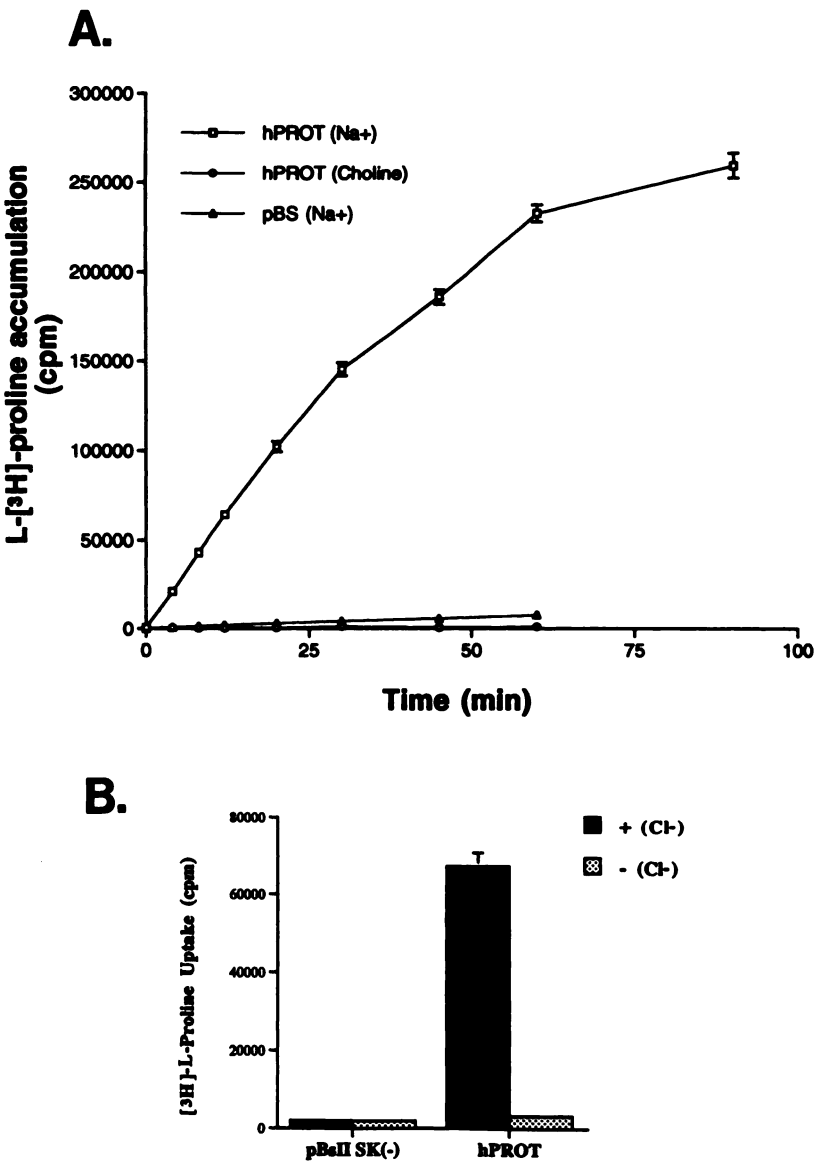


**Fig. 2.** $Na^+$, $Cl^-$, and time dependence of L-proline uptake in HeLa cells transfected with hPROT. A, Time course of L-[$^3$H]-proline accumulation into HeLa cells transfected with hPROT. $Na^+$ dependence was examined by isotonic substitution of assay NaCl with choline chloride. Background levels of proline transport were determined by transfecting HeLa cells under identical conditions with pBluescript SKII(−). Data represent the mean ± standard error of triplicate determinations. B, $Cl^-$ dependence of L-[$^3$H]-proline accumulation into HeLa cells transfected with hPROT. $Cl^-$ dependence was examined by isotonic substitution of assay NaCl with sodium gluconate. Data represent the mean ± standard error of triplicate determinations.

leucine, L-phenylalanine, *cis*-4-hydroxy-L-proline, L-azetidine-2-carboxylate, and *trans*-4-hydroxy-L-proline with the relative rank order of inhibition constants ($K_i$ values) of 12 μM, 24 μM, 28 μM, 30 μM, 36 μM, 65 μM, and 82 μM, respectively. Table 1 lists the compounds that exhibited $K_i$ values in excess of 100 μM.

**Brain-specific expression of hPROT.** To examine the pattern of expression of hPROT mRNA in human tissues, we hybridized a multiple tissue Northern blot at high stringency with a fragment of the hPROT cDNA (see "Materials and Methods"). Fig. 5 shows that a single prominent hybridizing species of ~4 kb was detected in poly($A^+$) mRNA from human brain. In addition, two higher molecular weight species were observed in human brain mRNA that may represent partially processed hnRNA. In contrast, no specific hybridizing species were observed in any of the peripheral tissues examined, including human heart, placenta, lung, liver, skeletal muscle, kidney, and pancreas. Furthermore, Fig. 5B shows that hPROT mRNA is heterogeneously distributed in different regions of human brain. The strongest hybridization signals were observed in hypothalamus and hippocampus. Moderate signals were observed in amygdala, thalamus, and subthalamic nucleus. In contrast, little or no specific hybridization was observed in the human corpus callosum, caudate nucleus, or substantia nigra.

To investigate the distribution of the hPROT protein in human tissues, an affinity-purified antipeptide antibody (C-597) was raised in rabbits against a 24-amino acid peptide from the carboxy-terminus of the predicted hPROT protein (18). This antibody specifically recognized a single 68-kDa PROT glycoprotein on immunoblots of rat and human brain tissues (18). Fig. 6 demonstrates that the hPROT protein is brain specific. Antibody C-597 recognized a single broad 68-kDa immunoreactive band in crude synaptosomal membranes from human brain (Fig. 6A) but not in membranes prepared from human liver, kidney, or heart (Fig. 6B). Immunorecognition of the 68-kDa band from human brain was completely blocked by preabsorption of antibody C-597 with a 20-fold excess of the carboxy-terminal antigen peptide but not with an unrelated 24-amino acid peptide or with protein extracts from liver (18). However, the ~74- and 49-kDa bands were labeled by Ab C-597 even in the presence of a

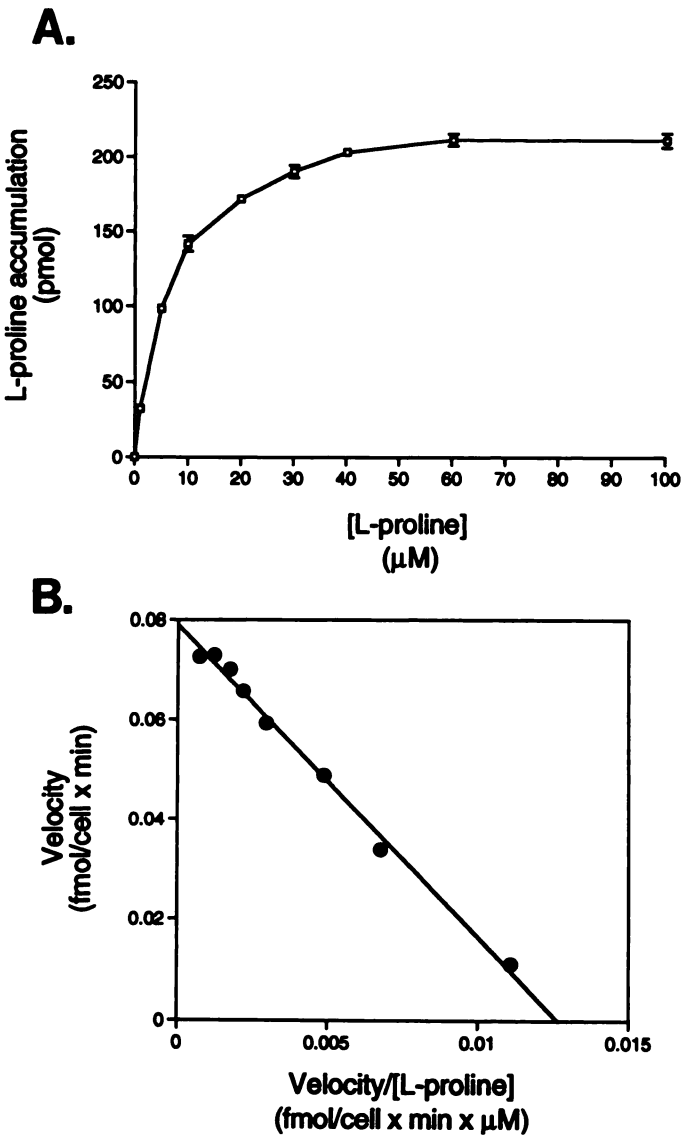


**Fig. 3.** Concentration dependence of L-proline uptake in HeLa cells transfected with hPROT. A, Uptake of 50 nM L-[$^3$H]-proline was determined in the presence of increasing concentrations of unlabeled L-proline during a 20-min incubation in transfected HeLa cells. Data represent the mean ± standard error of triplicate determinations. B, Eadie-Hofstee analysis of the data shown in A.

TABLE 1

**Compounds with $K_i$ values in excess of 100 μM**

HeLa cells (~125,000 per well) infected with $T_7$ RNA polymerase-containing vaccinia virus were transfected with hPROT (1 μg) and incubated with 50 nM L-[$^3$H]proline with or without 100 μM inhibitors for 20 min at 37° in triplicate.

| Proline analogs | Miscellaneous compounds | Amino acids |
|---|---|---|
| *N*-Acetyl-L-proline | 1-Aminocyclohexanecarboxylate | L-Alanine |
| *N*-Methyl-L-proline | 1-(Aminomethyl)-cyclohexaneacetate | L-Aspartate |
| L-Prolinamide | Carnosine | L-Cysteine |
| D-Proline | Cyclo-(His-Pro) | L-Glutamate |
| L-Prolinol | Cycloleucine | Glycine |
| L-Pyroglutamate | D-Cycloserine | L-Leucine |
| Pyrrole-2-carboxylate | 1-Cysteinesulphinate | L-Serine |
| Pyrrolidine | Histamine | L-Tyrosine |
| 2-Pyrrolidone | Isonipecotate | |
| | (±)-Nipecotate | |
| | Taurine | |
| | α-Aminoisobutyrate | |
| | α-Methylaminoisobutyrate | |
| | L-2,3-Diaminoproprionate | |
| | α-Ketoglutarate | |
| | L-Ornithine | |
| | L-β-Oxalylaminoalanine (BOAA) | |

20-fold excess of the specific peptide immunogen. Therefore, we conclude that the 68-kDa immunoreactive band represents the hPROT protein and that the 74- and 49-kDa bands represent background labeling.

When equal amounts of crude synaptosomal membranes (25 μg of protein per lane) from different regions of the same human brain were immunoblotted, a heterogeneous labeling pattern was observed (Fig. 6A). The most prominent immunoreactive bands were observed in hippocampus, corpus striatum, and temporal cortex. Immunoreactive bands of intermediate intensity were observed in frontal cortex and occipital cortex, whereas only weak labeling was observed in the cerebellum and parietal cortex. Prominent labeling of a single 68-kDa immunoreactive band was also observed with corpus striatum samples from two additional individuals (Fig. 6A). To demonstrate that equal amounts of protein were transferred from the SDS-PAGE gel to the nitrocellulose membrane, the membrane shown in Fig. 6A was stripped and reprobed with a rabbit polyclonal antibody directed against rat protein phosphatase inhibitor-1 (20). A prominent 27-kDa immunoreactive band was observed (labeled I-1; lanes 1–8 of bottom panel of Fig. 6A). During the stripping of the membrane, the region of the membrane containing lane 9 tore and was not reprobed.

**Chromosomal localization of the hPROT gene in human and mouse genomes.** The human chromosomal location of the hPROT gene was mapped by a combination of somatic cell hybrid DNA analysis and chromosomal *in situ* hybridizations (21). Southern blot analysis of DNA isolated from 18 human and rodent somatic cell hybrids mapped hPROT to human chromosome 5. The cDNA probe detected three human *Bgl* II fragments of 12.5, 7.2, and 1.7 kb; five mouse hybridizing bands of 13.5, 8.3, 5.8, 4.4, and 0.6 kb; and seven hamster fragments of 4.2, 3.4, 2.3, 1.7, 1.0, 0.55, and 0.3 kb (data not shown). The 1.7-kb fragment was indistinguishable in the human-hamster hybrid. All human-specific fragments segregated with chromosome 5 in 17 mouse-human hybrids scored. *In situ* hybridization of a tritium-labeled probe to human metaphase chromosome spreads confirmed the localization of the gene to chromosome 5 (Fig. 7A). Of 108 grains in 50 cells analyzed, 17 (15.7%) were located at 5q31–32. No other chromosomal site was labeled above background.

This region of human chromosome 5 contains a variety of genes encoding proteins involved in signal transduction and is homologous with regions of mouse chromosomes 11 and 18, to which neurological disorders have been mapped (reviewed in Ref. 25). Therefore, we determined the chromosomal location of the mouse PROT gene (designated *Prot*). A panel of DNA samples from an interspecific cross that has been characterized for genetic markers throughout the genome was analyzed (see Ref. 22). The genetic markers included in this map span 50–80 cM on each mouse autosome and the X chromosome. Hybridization of a 2.2 kb *Bam*HI/*Xba*I

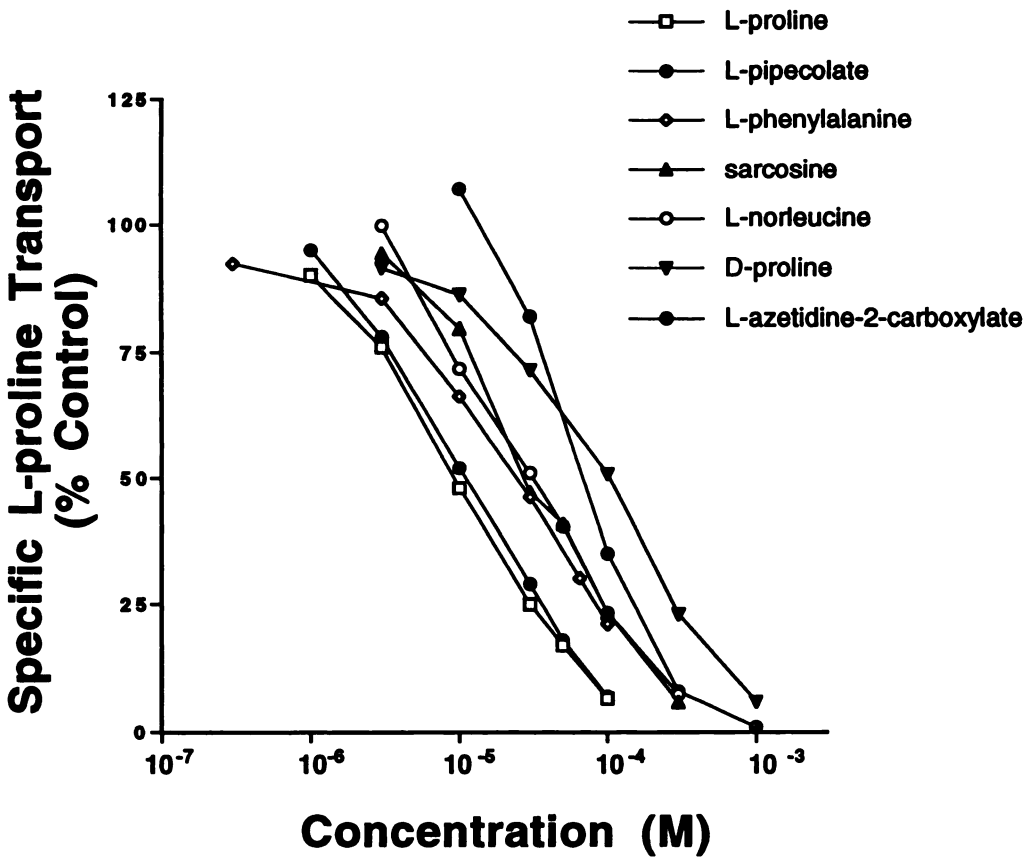


**Fig. 4.** Inhibition of proline transport by structural analogs in transfected cells. Proline transport assays (50 nM L-[$^3$H]-proline) were conducted for 20 min with or without increasing concentrations of the indicated pharmacological agents. Nonspecific transport was determined for each assay by a parallel transfection of pBluescript SKII(−) and values were subtracted from signals obtained with rPROT. Data represent triplicate determinations of the percentage of specific proline uptake obtained with labeled substrate alone.

fragment of rPROT to *Taq*I restriction endonuclease-digested DNA from the two parental mice defined informative RFLVs: C3H/HeJ-*gld*, 3.7, 3.5, 2.1, and 1.9 kb; and *Mus spretus*, 5.5 and 4.1 kb. Each of the restriction endonuclease-digested DNAs from the [(C3H/HeJ-*gld* × *Mus pretus*) F1 × C3H/HeJ-*gld*] interspecific backcross mice displayed either the homozygous or heterozygous $F_1$ pattern when hybridized with the cDNA probes, indicating that the RFLVs co-segregated.

Comparison of the haplotype distribution of the mouse PROT RFLVs among markers previously defined in this cross allowed *Prot* to be mapped to a specific position on mouse chromosome 18 (Fig. 7B). The best gene order ± the standard deviation indicated the following gene order from

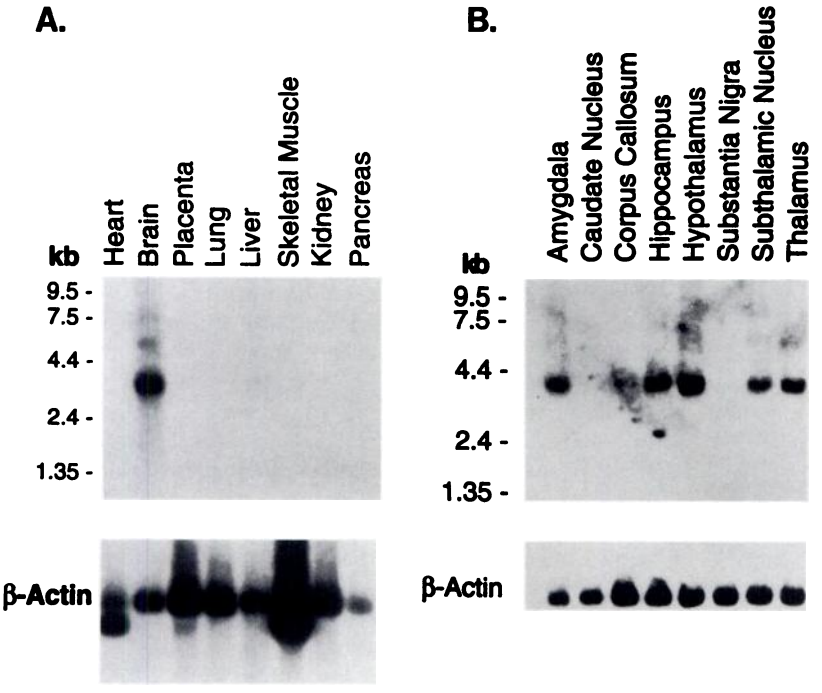


**Fig. 5.** Localization of hPROT mRNA in various human tissues. A, Brain-specific expression of hPROT mRNA shown in an autoradiograph (4 days) of hybridization of an hPROT cDNA probe to a human multiple tissue Northern blot (Clontech). B, Autoradiograph (1 week) of hybridization of an hPROT cDNA probe to a human brain multiple tissue Northern blot (Clontech).

proximal to distal on mouse Chr 18: *Grl1* (14.9 ± 3.3 cM), *Prot/Pdgfrb* (2.6 ± 1.5 cM), *Adrb2*.

## Discussion

**Brain-specific expression of hPROT.** We describe the isolation and characterization of cDNA clones for a hPROT. The cDNA sequence and deduced primary structure establish that this transporter represents the human homolog of a high affinity $Na^+$- (and $Cl^-$)-dependent PROT expressed in subpopulations of putative glutamatergic pathways in rat brain (17). We generated nucleic acid and immunological probes from the hPROT cDNA and undertook the first detailed investigation of the expression of hPROT mRNA and protein in human tissues. A prominent ~4-kb hPROT mRNA transcript was observed in human brain that exhibited a heterogeneous regional distribution (Fig. 5). In contrast, no specific hybridizing species were detected in peripheral tissue. Similarly, a single 68-kDa hPROT immunoreactive band was detected in crude synaptosomal membranes from various regions of human brain but not in membranes prepared from human liver, kidney, or heart. This apparent brain-specific expression of hPROT is interesting because other members of the GABA/norepinephrine transporter gene family do not show this degree of brain specificity. For example, multiple mRNAs arising from the hSERT have been detected in human placenta and lung in addition to serotonergic neurons in human brain (26, 27). Similarly, transcripts arising from the glycine transporter subtype GlyT-1, the GABA transporter subtypes GAT-2 and GAT-3, the taurine transporter, and the creatine transporter are widely expressed in peripheral tissues (reviewed in Ref. 19). We believe that the brain-specific expression of hPROT is consistent with an important physiological role for this transporter in the mammalian CNS.

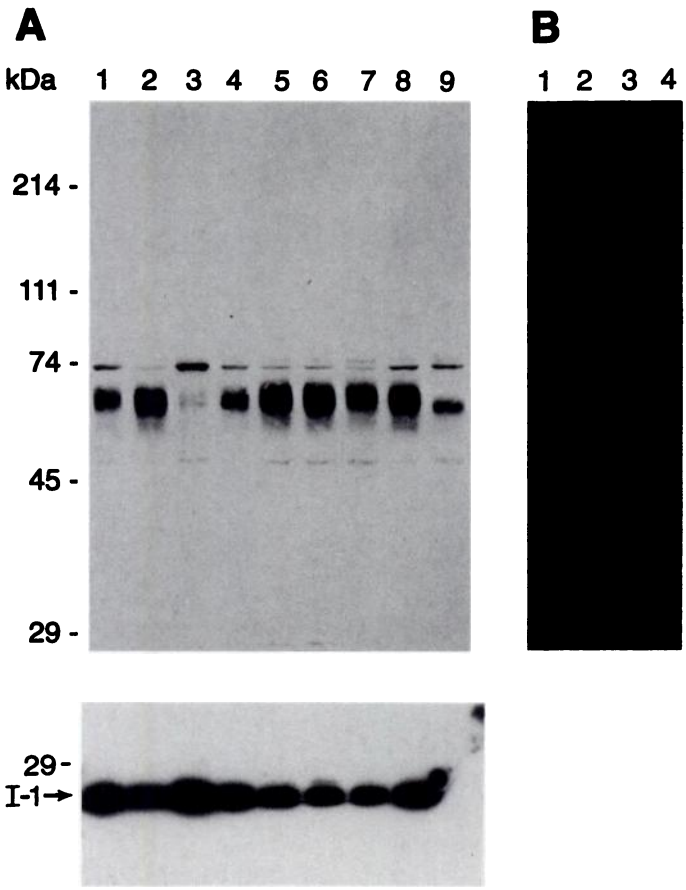


**Fig. 6.** Brain-specific expression of hPROT protein. A, *Top*, The distribution of the hPROT protein in the human CNS is shown. Crude synaptosomal membranes (25 μg of protein) from various human brain regions were subjected to SDS-PAGE and immunoblotted with anti-PROT antibody C-597 (0.01 μg/ml) as described (18) *Lane 1*, frontal cortex; *lane 2*, temporal cortex; *lane 3*, parietal cortex; *lane 4*, occipital cortex; *lane 5*, hippocampus; *lane 6*, corpus striatum; *lane 7*, corpus striatum; *lane 8*, corpus striatum; *lane 9*, cerebellum. The three corpus striatum samples shown in *lanes 6–8* were obtained from different individuals. *Bottom*, The membrane was stripped and reprobed with an affinity-purified antibody directed against protein phosphatase inhibitor-1 (20). A prominent 27-kDa immunoreactive band was observed in *lanes 1–8*. The portion of the membrane containing lane 9 tore during the stripping and was not reprobed. B, Lack of hPROT immunolabeling in peripheral tissues is shown. Human tissue homogenates (50 μg) derived from liver (*lane 1*), kidney (*lane 2*), heart (*lane 3*), and lung (*lane 4*) were subjected to SDS-PAGE and immunoblotted with anti-PROT antibody C-596 (0.01 μg/ml). *Left*, Mobility of prestained protein molecular weight markers.

We observed a differential distribution of hPROT mRNA and protein in the human corpus striatum. This brain region contains high levels of a 68-kDa hPROT immunoreactive protein (Fig. 6) but no detectable hPROT mRNA (Fig. 5). These results are consistent with the hypothesis that the hPROT protein is synthesized in neuronal cell bodies in an extrastriatal location and axonally transported to the corpus striatum. Similar results have been observed in rat brain (18). Rat striatal synaptosomes exhibit prominent high affinity $Na^+$-dependent L-proline uptake (5) and high levels of a 68-kDa immunoreactive rPROT protein (18). However, this brain region contains little or no rPROT mRNA (17, 18). Furthermore, our demonstration that rPROT mRNA is expressed by hippocampal CA3 pyramidal cells (17, 18) reinforces the conclusion of Nadler and colleagues from lesion (6) and uptake autoradiography (7) studies that high affinity $Na^+$-dependent L-proline uptake is enriched in terminal fields of the Schaffer collateral, commissural, and ipsilateral association projections of CA3 pyramidal cells. The prominent expression of rPROT mRNA in rat hippocampal CA3 pyramidal neurons (17, 18) is in striking contrast to the minimal uptake of [$^3$H]-L-proline over the CA3 pyramidal cell body layer compared with the corresponding axon terminal fields (Fig. 1 in Ref. 7). Taken together, these findings provide evidence for the axonal transport of the PROT protein. Future studies will use the C597 anti-PROT antibody in electron microscopic immunolabeling studies to examine whether mammalian brain PROT is localized to nerve terminals.

**Distinguishing features of mammalian brain PROT.** The pharmacological specificity, kinetic properties, and ionic requirements of hPROT clearly distinguish this carrier from the other $Na^+$-dependent plasma membrane carriers that transport L-proline, including the system "A" and system "ASC" neutral amino acid carriers (reviewed in Ref. 28) and the intestinal brush-border imino carrier (reviewed in Ref. 29). Mammalian brain PROT exhibits a $K_m$ of ~5–10 μM for L-proline uptake in transiently transfected HeLa cells, which is within the range of values reported previously for L-proline uptake by rat hippocampal synaptosomes ($K_m$ ~6–7 μM) (6). In contrast, the system "A", system "ASC," and imino carriers transport L-proline with low apparent affinity ($K_m$ values >230 μM) (see references in Ref. 28 and 29). Furthermore,

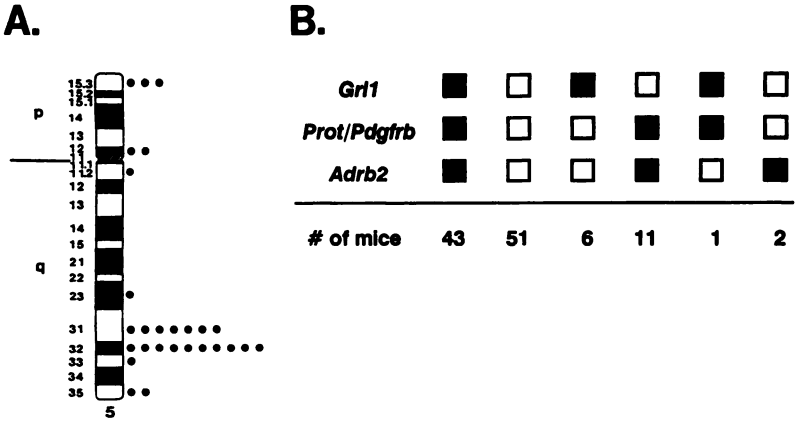


**Fig. 7.** Chromosomal localization of the PROT gene in human and mouse genomes. A, *In situ* chromosomal localization of the hPROT gene on human chromosome 5. The position and relative abundance of silver grains overlying human chromosome 5 are shown as determined by *in situ* hybridization of human metaphase chromosomes. B, Segregation of the *Lprot* locus on mouse chromosome 18 in [(C3H/HeJ-*gld* × *Mus spretus*) F1 × C3H/HeJ-*gld*] interspecific backcross mice. Filled boxes represent the homozygous C3H pattern, and open boxes represent the F1 pattern. For *Lprot*, informative *Taq*I restriction fragments were defined in the present study (C3H/HeJ-*gld*: 3.7, 3.5, 2.1, and 1.9 kb; and *Mus spretus* 5.5 and 4.1 kb). The name of each locus corresponds to the following gene: *Grl1*, glucocorticoid receptor 1; *Pdgfrb*, platelet-derived growth factor receptor-β; *Adrb2*, β2-adrenergic receptor.

mammalian brain PROT exhibits a narrow range of substrate specificity with striking selectivity for L-proline. In contrast, the system "A" and system "ASC" neutral amino acid carriers transport a wide range of neutral (dipolar) amino acids in addition to L-proline (see references in Ref. 28). Wright and Peerce (30) identified the rabbit intestinal brush-border imino carrier as a 100-kDa polypeptide on SDS-PAGE. In contrast, the mammalian brain PROT protein runs as a 68-kDa polypeptide (Fig. 6). Also, sarcosine (*N*-methylglycine) competes with high apparent affinity for hPROT-induced L-proline transport ($K_i$ ~24 μM) (Fig. 4) but only weakly inhibits L-proline transport by the rabbit jejunum brush-border imino carrier ($K_m$ ~8700 μM) (39).

Limited information is available describing the pharmacological properties of the native mammalian brain high affinity L-proline uptake system (4). In general, a good correlation exists between the potency of compounds in inhibiting the cloned human PROT transporter and L-proline uptake in brain slices (Table 1) (4). Thus, the open chain aliphatic compound L-norleucine is a potent inhibitor of both hPROT ($K_i$ ~24 μM) and L-proline uptake into rat cerebral cortical slices ($K_i$ ~20 μM [4]). However, the cyclic imino acid L-pipecolate is more potent at inhibiting mammalian brain PROT ($K_i$ ~12 μM) than L-proline uptake into rat cerebral cortical slices (DL-pipecolate ~$K_i$ 44 μM [4]). Also, L-azetidine-2-carboxylate is a more potent inhibitor of hPROT ($K_i$ ~82 μM) than of L-proline uptake into rat cerebral cortical slices ($K_i$ ~155 μM [4]).

Previously cDNAs were isolated that code for an *Escherichia coli K-12* $Na^+$/proline cotransporter that exhibits close homology at the DNA level and the predicted amino acid and secondary structure levels with human and rabbit intestinal $Na^+$/glucose cotransporters (reviewed in Ref. 31). Interestingly, although the *E. coli* $Na^+$/proline cotransporter and mammalian brain PROT both transport L-proline in a $Na^+$-dependent manner, no significant amino acid sequence homology exists between these two transporters, indicating that they must have evolved from distinct ancestral genes.

Based on studies of the inhibition of L-proline transport by structural analogs (Fig. 4 and Table 1), we are beginning to gain insights into the structural requirements for high affinity interaction of substrates and/or inhibitors with mammalian brain PROT. The ideal inhibitor must be the L-stereoisomer of a five- or six-member heterocyclic nitrogen containing a ring with an electronegative carboxylate group separated by one carbon atom from an electropositive tetrahedral imino nitrogen with two hydrogen atoms. Replacement of the carboxylate group of L-proline with —H (pyrrolidine), —$CH_2OH$ (L-prolinol), or =O (2-pyrrolidone) eliminated high affinity interaction with hPROT (Table 1). Furthermore, the inability of L-prolinamide to compete with high apparent affinity for L-proline transport suggests that the anionic nature of the carboxylate group is required for high affinity interaction with hPROT. The inability of *N*-methyl-L-proline to compete for L-proline transport establishes the requirement for a positively charged tetrahedral imino nitrogen with two hydrogen atoms for high affinity interactions with hPROT (Table 1). The importance of ring size is best illustrated by a comparison of the relative potency of the five-member L-proline ($K_i$ ~6 μM) versus the six-member L-pipecolate ($K_i$ ~14 μM) versus the four-member L-azetidine-2-carboxylate ($K_i$ ~65 μM). The order-of-magnitude decrease in potency of L-azetidine-2-carboxylate most likely reflects the lack of conformational flexibility of the strained four-member heterocyclic ring, which prevents the imino nitrogen, carboxylate group, and hydrophobic region from assuming a favorable position for interaction with the transporter (reviewed in Ref. 39). Optimal spacing of the imino nitrogen and the carboxylate group is crucial for high affinity interaction with hPROT. This is best illustrated by the relative potency of L-pipecolate ($K_i$ ~14 μM) versus (±)-nipecotate or isonipecotate ($K_i$ values ≫100 μM) (Fig. 4 and Table 1). Moving the carboxylate residue from position 2 (L-pipecolate) to position 3 ((±)-nipecotate) or 4 (isonipecotate) eliminates high affinity interactions with hPROT. Finally, although cyclic imino acids have the highest affinity for hPROT, the aliphatic imino acid sarcosine (*N*-methylglycine) and the aliphatic amino acid L-norleucine display moderately high apparent affinity for hPROT: $K_i$ values of 24 μM and 28 μM, respectively (Fig. 4). The relatively free rotation about the nitrogen/carbon bonds in these aliphatic carboxylates may permit these molecules to assume a conformation that resembles the more stable, puckered ring of L-proline (39).

**Potential physiological role(s) of high affinity L-proline uptake in the mammalian CNS.** Because mammalian brain PROT presumably serves to translocate L-proline from the extracellular fluid into the cytoplasm of neurons that express this carrier, high affinity uptake could serve to reduce the extracellular fluid L-proline concentration and/or to provide an intracellular pool of L-proline. It may be important to limit the concentration of L-proline in brain interstitium to

ensure that this imino acid does not reach levels that would inappropriately activate L-glutamate and/or strychnine-sensitive glycine receptors (12). Alternatively, if L-proline has a novel chemical signaling role in the mammalian CNS, then high affinity uptake could regulate the concentration and duration of the putative synaptic pool of L-proline and/or conserve L-proline for re-use.

High affinity L-proline uptake could have an unprecedented metabolic or osmotic role in neurons. In this regard, recent findings in honeybees and *Drosophila* indicate that there is an important metabolic link between L-proline and L-glutamate in nervous tissue. Tsacopoulos and colleagues (32) observed that honeybee photoreceptor mitochondria respond to light stimulation by rapidly oxidizing L-proline to L-glutamate. They propose that this newly synthesized L-glutamate then enters the Krebs' cycle as $\alpha$-keto-glutarate through a reaction catalyzed by glutamate dehydrogenase. According to their model, L-proline uptake could serve to fuel photoreceptor neurons by increasing the supply of Krebs' cycle intermediates that might otherwise become depleted during prolonged photostimulation. By analogy, high affinity L-proline uptake could provide a metabolic fuel for mammalian nerve terminal mitochondria.

Recently, Hayward and colleagues (33) discovered that a mutation in the mitochondrial proline oxidase gene of *Drosophila melanogaster* results in abnormal locomotor behavior characterized by sluggish motor activity and wing fluttering. Proline oxidase catalyzes the first step in the catabolism of L-proline to L-glutamate (34). Interestingly, L-glutamate is the neuromuscular transmitter in *Drosophila* (33). Therefore, a deficiency in mitochondrial proline oxidase may alter the synthesis and/or release of the transmitter pool of L-glutamate in specific nerve cell populations in *Drosophila*. Similarly, rat brain synaptosomes metabolize L-proline to L-glutamate through the sequential actions of proline oxidase and delta-1-pyrroline-5-carboxylate dehydrogenase (34). However, these enzymes are believed to exist in glial cells, not neurons (see references in Ref. 17). Future studies are necessary to determine the metabolic fate of the L-proline taken up through the high affinity mammalian brain PROT.

High affinity $Na^+$-dependent transport processes also mediate the presynaptic accumulation of certain neurotransmitter precursors. For example, the rate-limiting step in the biosynthesis of acetylcholine is believed to be $Na^+$-dependent choline uptake into cholinergic nerve terminals by a hemicholinium-sensitive high affinity choline transporter (35). By analogy, high affinity L-proline uptake by selected nerve terminals may provide a precursor pool of L-proline for the synthesis of a novel neurotransmitter.

Finally, neurotransmitter transporters can operate in reverse, pumping neurotransmittters out of cells and serving as a $Ca^{2+}$-independent nonvesicular mechanism for neurotransmitter release (reviewed in Ref. 36). It is therefore conceivable that reversal of the PROT during neuronal depolarization may provide a mechanism for the $Ca^{2+}$-independent nonvesicular release of L-proline. Because L-proline can be neurotoxic (14), such a mechanism could contribute to the neuronal death associated with brain anoxia.

**Implications of chromosomal localization.** The PROT gene was localized to human chromosome 5q31–32. Although no human neurological disorders have been mapped to this region, 5q31–32 has homologies with regions of mouse chromosomes 11 and 18, to which neurological disorders have been mapped (25). High-resolution mapping of the murine *Prot* gene locus allowed assignment of *Prot* to 14.9 cM distal to *Grl1* and 2.6 cM proximal to *Adrb2* on mouse chromosome 18. Interestingly, the mouse neurological disorder *bouncy* maps to this region of mouse chromosome 18 (37). *Bouncy* is a recessive mutation in which homozygotes can be recognized by their small size, severe tremor, and bouncy gait when moving. The molecular basis of this disorder is unknown. Because *Prot* and *bouncy* map to the same region of mouse chromosome 18, future studies are warranted to determine whether mutations in the PROT result in the murine *bouncy* phenotype. Finally, the chromosomal localization of *Prot* in the mouse is consistent with the mapping of the human homolog to the long arm of human chromosome 5 (5q31–32).

In conclusion, we have isolated and characterized cDNAs that code for a high affinity $Na^+$- (and $Cl^-$)-dependent PROT from human brain. The pharmacological specificity, kinetic properties, and ionic requirements of hPROT clearly distinguish this carrier from the other $Na^+$-dependent plasma membrane carriers that transport L-proline. The brain-specific expression of hPROT mRNA and protein together with our evidence for the axonal transport of the PROT protein warrant the consideration of a synaptic regulatory role(s) for this transporter and its presumed natural substrate L-proline in the mammalian CNS. To facilitate studies of the physiological role(s) of high affinity L-proline transport in nervous tissue, it would be desirable to develop a high affinity antagonist of mammalian brain PROT. It is striking that few pharmacological agents exist that selectively antagonize the transport of specific amino acid neurotransmitters by their cognate transporters. The development of selective inhibitors of amino acid neurotransmitter transporters may represent a fertile area for the development of novel therapeutic agents for treating neuropsychiatric disorders.

#### Acknowledgments

We gratefully acknowledge Dr. John R. Gilbert and the Joseph and Kathleen Bryan Alzheimer's Disease Research Center, Division of Neurology, Duke University Medical Center, Durham, NC, for the provision of human brain and peripheral tissues.

#### References

1. Yoneda, Y., and E. Roberts. A new synaptosomal biosynthetic pathway of proline from ornithine and its negative feedback inhibition by proline. *Brain Res.* **239:**479–488 (1982).
2. Bennett, J. P., W. J. Logan, and S. H. Snyder. Amino acid neurotransmitter candidates: sodium-dependent high affinity uptake by unique synaptosomal fractions. *Science* **178:**997–999 (1972).
3. Peterson, N. A., and E. Raghupathy. Characteristics of amino acid accumulation of synaptosomal particles isolated from rat brain. *J. Neurochem.* **19:**1423–1438 (1972).
4. Balcar, V. J., G. A. R. Johnston, and A. L. Stephenson. Transport of L-proline by rat brain slices. *Brain Res.* **102:**143–151 (1976).
5. Hauptmann, M., D. F. Wilson, and M. Erecinska. High affinity proline uptake in rat brain synaptosomes. *FEBS Lett.* **161:**301–305 (1983).
6. Nadler, J. V. Sodium-dependent proline uptake in the rat hippocampal formation: association with ipsilateral commissural projections of CA3 pyramidal cells. *J. Neurochem.* **49:**1155–1160 (1987).
7. Nadler, J. V., S. D. Bray, and D. A. Evanson. Autoradiographic localization of proline uptake in excitatory hippocampal pathways. *Hippocampus* **2:**269–278 (1992).
8. Bennett, J. P., A. H. Mulder, and S. H. Snyder. Neurochemical correlates of synaptically active amino acids. *Life Sci.* **15:**1945–1056 (1974).
9. Nickolson, V. J. "On" and "off" responses of $K^+$-induced synaptosomal proline release: involvement of the sodium pump. *J. Neurochem.* **38:**289–292 (1982).
10. Greene, W. M., A. Wang, and J. V. Nadler. Sodium-independent binding of

L-[$^3$H]proline to hippocampal synaptic membranes. *Eur. J. Pharmacol.* **130**:333–336 (1986).
11. Cordero, M. L., A. E. Negron, J. G. Ortiz, C. Blanco, and G. Santiago. Inhibition of high affinity [$^3$H]-L-proline binding to rat brain membranes by 2-amino-7-phosphonoheptanoic acid. *Eur. J. Pharmacol.* **208**:179–181 (1991). .
12. Henzi, V., D. B. Reichling, S. W. Helm, and A. B. MacDermott. L-Proline activates glutamate and glycine receptors in cultured rat dorsal horn neurons. *Mol. Pharmacol.* **41**:793–801 (1992).
13. Keller, E., J. L. Davis, K. H. Tachiki, J. T. Cummins, and C. F. Baxter. L-Proline inhibition of glutamate release. *J. Neurochem.* **37**:1335–1337 (1981).
14. Nadler, J. V., A. Wang, and A. Hakim. Toxicity of L-proline toward rat hippocampal neurons. *Brain Res.* **456**:168–172 (1988).
15. Cherkin, A., M. J. Ickardt, and L. K. Gerbrandt. Memory: proline induces retrograde amnesia in chicks. *Science* **193**:242–244 (1976).
16. Phang, J. M., and C. R. Scriver. Disorders of proline and hydroxyproline metabolism, in *The Metabolic Basis of Inherited Disease* (C. R. Scriver, A. L. Beaudet, W. S. Shy, and D. Valle, eds.). McGraw-Hill, New York, 577–597 (1989).
17. Fremeau, R. T., M. G. Caron, and R. D. Blakely. Molecular cloning and expression of a high affinity L-proline transporter expressed in putative glutamatergic pathways of rat brain. *Neuron* **8**:915–926 (1992).
18. Velaz-Faircloth, M., A. Guadano-Ferraz, V. Henzi, and R. T. Fremeau, Jr. Mammalian brain-specific L-proline transporter: neuronal localization of mRNA and enrichment of transporter protein in synaptic plasma membranes. *J. Biol. Chem.*, **270**:15755–15761 (1995).
19. Shafqat, S., M. Velaz-Faircloth, A. Guadano-Ferraz, and R. T. Fremeau, Jr. Molecular characterization of neurotransmitter transporters. *Mol. Endocrinol.* **7**:1517–1529 (1993).
20. Elbrecht, A., J. DiRenzo, R. G. Smith, and S. Shenolikar. Molecular cloning of protein phosphatase inhibitor-1 and its expression in rat and rabbit tissues. *J. Biol. Chem.* **265**:13415–13418 (1990).
21. Yang-Feng, T. L., G. Floyd-Smith, M. Nemer, J. Drouin, and U. Francke. The pronatriodilatin gene is located on the distal short arm of human chromosome 1 and on mouse chromosome 4. *Am. J. Hum. Genet.* **37**:1117–1128 (1985).
22. Seldin, M. F., H. C. Morse III, J. P. Reeves, C. L. Scribner, R. C. LeBoeuf, and A. D. Steinberg. Genetic analysis of autoimmune *gld* mice: 1. identification of a restriction fragment length polymorphism closely linked to the *gld* mutation within a conserved linkage group. *J. Exp. Med.* **167**:688–693 (1988).
23. Kennelly, P. J., and Krebs, E. G. Consensus sequences as substrate specificity determinants for protein kinases and protein phosphatases. *J. Biol. Chem.* **266**:15555–15558 (1991).
24. Kuhar, M. J., and M. A. Zarbin, M. A. Synaptosomal transport: a chloride dependence for choline, GABA, glycine and several other compounds. *J. Neurochem.* **31**:251–256 (1978).
25. McNamara, J. O., J. H. Eubanks, J. D. McPherson, J. J. Wasmuth, G. A. Evans, and S. A. Heinemann. Chromosomal localization of human glutamate receptor genes. *J. Neurosci.* **12**:2555–2562 (1992).
26. Ramamoorthy, S., A. L. Bauman, K. R. Moore, H. Han, T. L. Yang-Feng, A. S. Chang, V. Ganapathy, and R. D. Blakely. Antidepressant- and cocaine-sensitive human serotonin transporter: molecular cloning, expression, and chromosomal localization. *Proc. Natl. Acad. Sci. USA* **90**:2542–2546 (1993).
27. Austin, M. C., C. C. Bradley, J. J. Mann, and R. D. Blakely. Expression of serotonin transporter mRNA in the human brain. *J. Neurochem.* **62**:2362–2367 (1994).
28. Christensen, H. N. Role of amino acid transport and countertransport in nutrition and metabolism. *Physiol. Rev.* **70**:43–77 (1990).
29. Stevens, B. R., Kaunitz, J. D., and Wright, E. M. Intestinal transport of amino acids and sugars: advances using membrane vesicles. *Annu. Rev. Physiol.* **46**:417–433 (1984).
30. Wright E., and B. E. Peerce. Identification and conformational changes of the intestinal proline carrier. *J. Biol. Chem.* **259**:14993–14996 (1984).
31. Hediger, M. A., E. Turk, and E. M. Wright. Homology of the human intestinal $Na^+$/glucose and Escherichia coli $Na^+$/proline cotransporters. *Proc. Natl. Acad. Sci. USA* **86**:5748–5752 (1989).
32. Tsacopoulos, A. L. Veuthey, S. G. Saravelos, P. Perrottet, and G. Tsoupras. Glial cells transform glucose to alanine, which fuels the neurons in the honeybee retina. *J. Neurosci.* **14**:1339–1351 (1994).
33. Hayward, D. C., S. J. Delaney, H. D. Campbell, A. Ghysen, S. Benzer, A. B. Kasprzak, J. N. Costell, I. G. Young, and G. L. Miklos. The sluggish-A gene of Drosophila melanogaster is expressed in the nervous system and encodes proline oxidase, a mitochondrial enzyme involved in glutamate biosynthesis. *Proc. Natl. Acad. Sci. USA* **90**:2979–2983 (1993).
34. Johnson, J. L., and E. Roberts. Proline, glutamate, and glutamine metabolism in mouse brain synaptosomes. *Brain Res.* **323**:247–256 (1984).
35. Kuhar, M. J., and L. C. Murrin. Sodium-dependent, high affinity choline uptake. *J. Neurochem.* **30**:15–21 (1978).
36. Attwell, D., B. Barbour, and W. Szatkowski. Nonvesicular release of neurotransmitter. *Neuron* **11**:401–407 (1993).
37. Johnson, K. R., and M. T. Davisson. Mouse chromosome 18. *Mammalian Genome* **5**:S259–265 (1994).
38. Karp, S. J., M. Masu, T. Eki, K. Ozawa, and S. Nakanishi. Molecular cloning and chromosomal localization of the key subunit of the human N-methyl-D-aspartate receptor. *J. Biol. Chem.* **268**:3728–3733 (1993).
39. Stevens, B. R., and E. M. Wright. Substrate specificity of the intestinal brush-border proline/sodium (imino) transporter. *J. Membrane Biol.* **87**: 27–34 (1985).
40. Bishop, D. T. The information content of phase-known matings for ordering genetic loci. *Genet. Epidemiol.* **2**:349–361 (1985).

**Send reprint requests to:** Robert T. Fremeau, Jr., Ph.D., Department of Pharmacology, Duke University Medical Center, Box 3813, Durham, NC 27710.